Science of the Total Environment 811 (2022) 152375

Contents lists available at ScienceDirect

Science of the Total Environment

journal homepage: www.elsevier.com/locate/scitotenv

# Tunneling-induced groundwater depletion limits long-term growth dynamics of forest trees

Hamid M. Behzad [a], Yongjun Jiang [a,*], Muhammad Arif [b], Chao Wu [a], QiuFang He [a], Haijuan Zhao [a], Tongru Lv [a]

[a] Chongqing Key Laboratory of Karst Environment & School of Geographical Sciences, Southwest University, Chongqing 400715, China
[b] Key Laboratory of Eco-Environments in the Three Gorges Reservoir Region (Ministry of Education), Chongqing Key Laboratory of Plant Resource Conservation and Germplasm Innovation, School of Life Sciences, Southwest University, Chongqing 400715, China

## HIGHLIGHTS

- Tunneling-induced groundwater depletion (TIGD) affects forest growth significantly.
- Tree-ring data can be used to monitor TIGD-related ecohydrological effects.
- Climate-caused growth pulses were differentiated from tunneling-induced growth pulses.
- Responses to TIGD were both cumulative and profound over time.
- Tunneling has more adverse effects on forest growth dynamics than drought.

## GRAPHICAL ABSTRACT

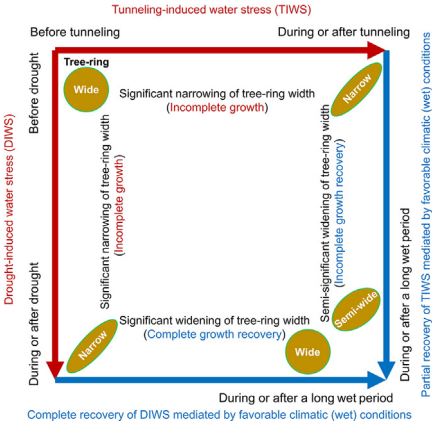


## ARTICLE INFO

*Article history:*
Received 3 October 2021
Received in revised form 29 November 2021
Accepted 9 December 2021
Available online 13 December 2021

Editor: Fernando A.L. Pacheco

*Keywords:*
Tree-ring width records
Tree growth dynamics
Tunnel construction
Groundwater depletion
Drought
Mountainous forest ecosystem

## ABSTRACT

Human interventions such as tunnel construction have caused groundwater depletion, which substantially affected the functions of forest tree species and their communities. However, the extent to which tunneling-induced groundwater depletion (TIGD) degrades their function levels at various spatial-temporal scales under varying climate conditions remains still unclear. Researchers used stand-scale dendrological records to track and extract the effects of TIGD associated with a single or series of tunneling events (three tunneling events during 1999–2001, 2006–2008, and 2010–2013) on short- and long-term growth levels of two dominant drought-tolerant tree species across (karst and non-karst) landscapes affected by tunnel construction and landscapes not subjected to tunnel construction in a mountainous forest ecosystem located in the southwest of China. The results showed that growth responses of both trees stand to TIGD, and the TIGD-linked water losses of other available water sources were negative and widespread across tunnel-affected landscapes, particularly in the karst landscapes known as delicate landscapes. Tree stands with faster (more vigorous) growth rates showed more significant adverse growth levels in response to either tunneling-induced or drought-induced water stresses. Also, they showed the highest recovered growth levels in response to favorable climatic conditions. Moreover, the growth level in the tunnel-affected forest never fully recovered during six years of very wet weather (2012–2018) after the construction of the final (third) tunnel in 2010–2013. Current research shows that tunnel construction has a cumulatively detrimental impact on the long-term survival of the forest. Even with the mediation of long-term very wet circumstances, it can substantially restrict the development dynamics of the forest compared to drought.

* Corresponding author.
*E-mail address:* jiangjyj@swu.edu.cn (Y. Jiang).

http://dx.doi.org/10.1016/j.scitotenv.2021.152375

## 1. Introduction

Over the last three decades, urban expansion and economic development worldwide have been indebted to the development of basic infrastructures, such as tunnels (Zhao et al., 2013; Lv et al., 2020). To date, although many efforts have been made to construct kilometers of tunnels for multipurpose projects (Lv et al., 2020), the underlying challenges associated with their construction are still not well understood. In most ecosystems affected by tunneling, especially in delicate ecosystems like karst, since tunnels are often excavated below the water table, the most commonly reported problem is groundwater depletion (Cesano et al., 2000; Celico et al., 2005; Attanayake and Waterman, 2006; Butscher et al., 2011; Chiu and Chia, 2012; Li et al., 2016). This may, in turn, lead to a sizable drawdown in the groundwater table and, thus, influence the regional hydrologic cycle (Vincenzi et al., 2009; Butscher et al., 2011). Besides, it may bring cascading effects with irreversible and even devastating consequences on ecosystem function. Among these effects, it can be mentioned a depletion and degradation of all water resources (for example, surface water and soil water) in any ecosystem and cutting off connections across them with groundwater (Vincenzi et al., 2009); or a reduction in water uptake or shift in water-use strategies of plants (Liu et al., 2019). The latter, in turn, may lead to a decrease in growth rate (Zheng et al., 2017) and even plant death (Lei et al., 2010). Therefore, any change in the groundwater flow field or any perturbation to the water balance of relevant ecosystems may seriously degrade the life of plants, especially groundwater-dependent plants (Li et al., 2018; Gokdemir et al., 2019).

Previous studies have mostly focused on the direct effects of tunneling-induced groundwater depletion (TIGD), such as water inrush into the tunnel (Li and Kagami, 1997; Perrochet, 2005; Kolymbas and Wagner, 2007; Vincenzi et al., 2014), contamination of urban groundwater (Chae et al., 2008; Banzato et al., 2011; Mossmark et al., 2015), and geological hazards (Casagrande et al., 2005; Pujades et al., 2015; Chen et al., 2017; Zeng et al., 2019). However, there is still limited comprehensive and systematic research on ecohydrological feedback and its effects. For instance, it remains unclear to what extent TIGD may influence the forest ecosystem's short- and long-term function at the stand and landscape scales. Whether can climate mediate (alleviate or exacerbate) the ecohydrological (negative) effects resulting from TIGD. To address and respond to these questions, proxy indicators, such as tree growth pulses (extracted from tree-ring width records) signaling to pulsed source water availability for plant water uptake, are essentially needed (Creutzfeldt et al., 2015; Edvardsson and Hansson, 2015; Tamkeviciute et al., 2018). This is primarily because continuous measurements of groundwater levels (as well as storage dynamics of other plant-available water-source pools) are sparse, and—if existing at all—they are too short. Thus, this study was attempted to show how unstandardized basal area increment (BAI) series from two dominant drought-tolerant tree species (Masson pine and Camphor laurel) across a mountainous forest ecosystem could be used as a proxy indicator. This technique was supposed to be efficient and useful to track the growth responses of the forest stands to hydrological variability resulting from TIGD of individual tunneling events under contrasting climate extremes and also to quantitatively estimate the degree of their short- and long-term growth responsiveness to a single or a collection of tunneling events. BAI series were derived from tree ring-width measurements using the method described by Jump et al. (2006) (see Materials and Methods). Given the inseparable relationship between climate and growth (Fritts, 1976; Lloyd, 1997; Grace et al., 2002; Lebourgeois et al., 2005; Jump et al., 2006; Yu et al., 2013; Fkiri et al., 2018; Kukarskih et al., 2020), it might be hard to differentiate tunneling-induced growth pulses from climate-caused growth pulses. Thus, before addressing how to disentangle these pulses from each other, there was a need to extract and analyze the climate effects on the growth trend. For this purpose, different approaches were used, including response function analysis, standardization procedures, and climatic indices, detailed descriptions of which can be found in the Methods.

We focused our study on an exemplar tunnel-affected forest site (Longfeng trough valley) and an exemplar tunnel-unaffected forest site (Longche trough valley) across a mountainous area (Zhongliang Mountain; a forest mountainous covered with mixed evergreen broad-leaved trees) located in Chongqing, Southwest of China (Fig. 1). At different time intervals of 1999–2001, 2006–2008, and 2010–2013, three tunnels approximately 4-km long were constructed in the Longfeng trough valley to develop urban transportation systems. These tunnels connected remote areas of the Chongqing metropolitan region blocked by the Zhongliang Mountain to its central region. All the three tunnels passed through aquifers formed in the karst and non-karst landscapes, which led to significant groundwater depletion during the excavation phase of each tunnel (Table S1). Observational pieces of evidence available during tunneling events have documented that the volume of groundwater released into the tunnels for the karst aquifer was far higher than that of the non-karst aquifer (Liu et al., 2019; Li et al., 2020). Accordingly, several karst and non-karst plots were selected for tree sampling within the affected site. Adjacent to the tunnel-affected site, the Longche trough valley is a pristine forest site, without any clear signs of anthropogenic interventions such as tunnel construction. Therefore, we considered it as a valuable comparative model for extracting and visualizing the tunneling-induced ecohydrological effects in the affected forest site. Although this site was geologically, hydrologically, and hydrogeologically similar to the affected site, it might never have been affected by the three above-mentioned tunneling events for the following reasons. First, there is a hydrological divide line between the affected and unaffected sites, suggesting that these sites' groundwater (including underground rivers) and surface water systems were not connected to each other either during or after establishing all three tunnels. Therefore, the hydrological divide line was considered as a basic criterion for demarcating these two sites from each other (Fig. 1). Second, unlike the affected site, the discharge rates of springs and wells across the unaffected site did not show any remarkable changes after excavation or establishing tunnels (Liu et al., 2019; Li et al., 2020). Thus, for these reasons, it was supposed that, unlike the affected site, forest growth conditions in the unaffected site had not been affected due to TIGD. Overall, the tunnel-affected forest site was selected in light of the above-mentioned research objectives and the multidimensional significance, including: (1) ecohydrological situations and feedbacks (affected by tunneling events) observed in this site may typify many similar tunnel-affected forest ecosystems in the regional, national, and global scales; (2) karst landscapes in the region have shown substantial heterogeneity and large temporal and spatial variability than the non-karst landscapes in relation to interactions between forest stands, climate, and water resources (Cao et al., 2020; Li et al., 2020; Wu et al., 2021), representing a broad range of ecohydrological feedbacks to be compared in similar landscapes; (3) existence of a pristine forest site with similar settings in its adjacent as a valuable comparative model, as explained above; and (4) a series of primary studies and field observations of short-term plant–source water relations and key ecohydrological processes were available for both affected and unaffected forest sites (Liu et al., 2019; Cao et al., 2020; Wu et al., 2021).

## 2. Materials and methods

### 2.1. Study site: Longfeng and Longche trough valleys

The Longfeng and Longche trough valleys are located within the northern part of the Zhongliang Mountain, northwest of Chongqing, southwest China, with surface areas of ~12 and ~27 $km^2$, respectively (29°39′05″-29°49′02″N, 106°23′15″-106°28′05″E, Fig. 1). The study site is mostly covered with mixed evergreen broad-leaved trees, including Chinese fir (*Cunninghamia lanceolata*), Camphor laurel (*Cinnamomum camphora*), Masson pine (*Pinus massoniana*), and Schima superba (*Chinese Gardn. and Champ.*) as dominant tree species. Most of the tree species were aerially seeded in the middle of the 1990s, and thus are young and single-age with over 30 years old. Climatologically, the study site has a humid subtropical monsoon climate with a 30-year mean annual rainfall of ~1100 mm. Annual rainfall distribution in the region is characteristically uneven throughout the year. Rainfall mostly occurs between May and October

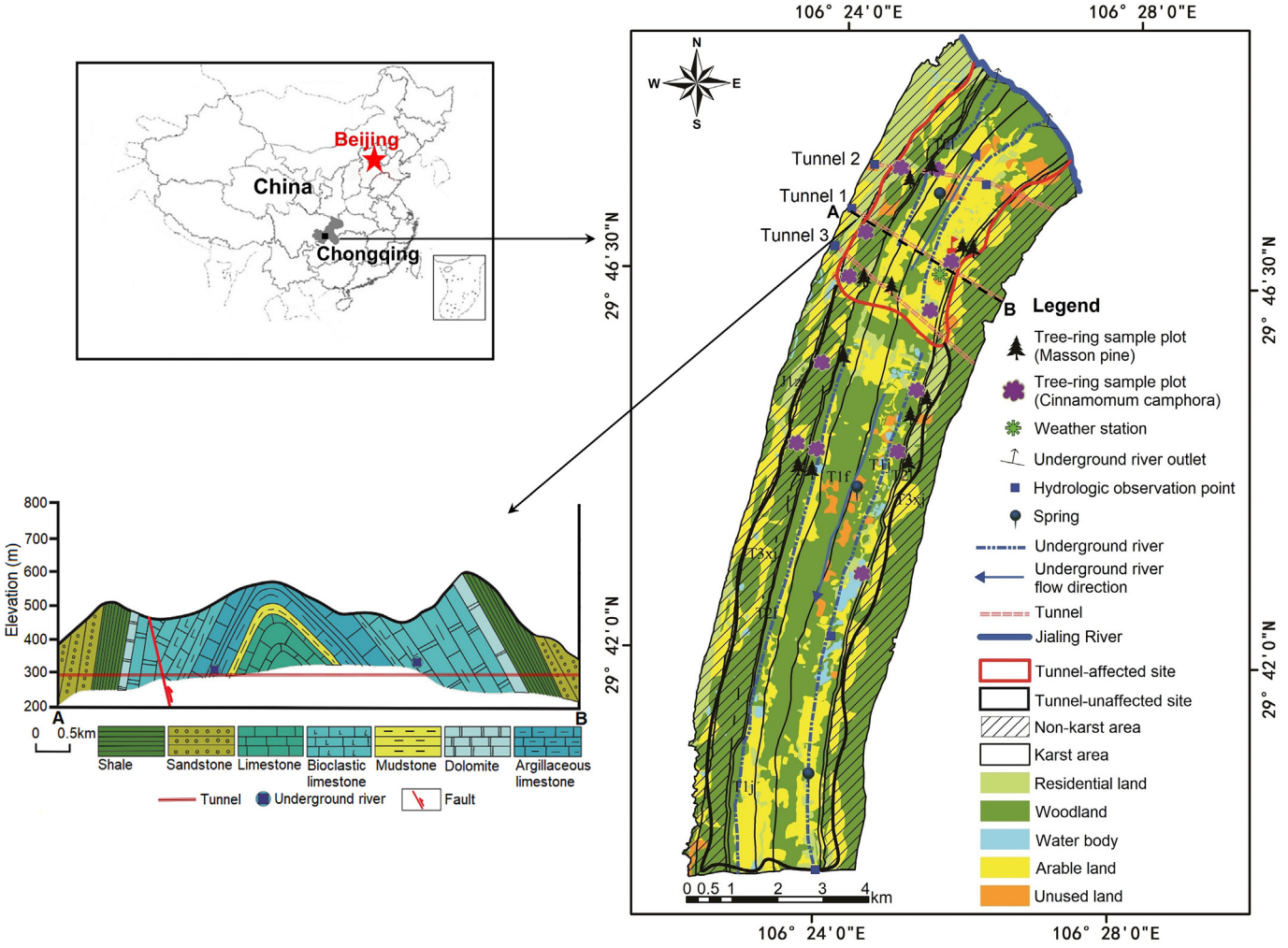


**Fig. 1.** Location, hydrology, land use/cover, and tree-ring sample plots/sites. The left-upper inset map shows the geographic location of the study site in the Zhongliang Mountain, northwest of Chongqing, southwest China. The left-lower inset map shows a geological cross-section in the tunnel-affected site (Longfeng trough valley).

during the growing season, accounting for ~75–85% of the total annual rainfall. The 30-year mean annual temperature equals 18.2 °C, with monthly average minimum and maximum temperatures of 5.9 and 33.6 °C in January and August.

Geological surveys have shown that the valleys were formed in well-developed karst limestone with a thickness of 500–700 m and are surrounded on two sides by non-karst (sandstone and mudstone) ridges with a thickness of 170–1100 m. In addition to the karst valleys, the study site has various karst features, including open crevices, sinkholes, shafts at the surface, channel conduits, small caverns, and underground rivers (or cave streams) at depth. Features of the surface karst provide fast transfer of rainwater and surface water into karst aquifers below and ultimately to underground rivers, limiting water storage of plant-available water-source pools in the shallow zones (Rong et al., 2011; Estrada-Medina et al., 2013; Yang et al., 2016). Before 2000, there were numerous karst springs and wells in the Longfeng valley, which supplied water for drinking and irrigation in the region. However, at the beginning of the first tunnel construction (1999–2001), most of them dried up. Additionally, for this reason, surface streams gradually depleted, which led to a large drop in the discharge of two underground rivers in the Longfeng trough valley. The previous work can follow details on the study area (Liu et al., 2019).

### 2.2. Sampling design, data collection, and analyses

Two of the most common species of (drought-tolerant) tree stands in the study site, including Masson pine and Camphor laurel (here abbreviated as pine and camphor), were selected for sampling. Choosing two different species of tree stands might have been important for at least two reasons. First, because of genetic differences among tree species, there is a varying degree of stress-driven responses (or resistance) for each species of tree stands even if growth conditions (that is, site quality) are similar to them (Hann and Larsen, 1991; Bowman et al., 2013). For instance, faster-growing tree species, such as camphor was likely to have stronger and more prevalent responses to water stress resulting from tunneling and climate events than slower-growing tree species, such as pine (Bigler and Veblen, 2009; Rozendaal et al., 2010). Consequently, it was assumed that the degree of growth responsiveness to stress-driven events would not be the same among each of these tree stands. Second, signals linked to non-climatic perturbations, such as tunneling, either might not have been perfectly captured by a single species of tree stands in a forest ecosystem or might have been exacerbated or alleviated under drought and wet climate extremes. Thus, there was a need to select at least two different tree stand species to reduce uncertainties and draw more reliable conclusions regarding the ecohydrological consequences of tunnel construction in the study area. For sampling each tree stand, six 1- to 1.5-ha plots (3 karst plots vs. 3 non-karst plots) were randomly established across both affected and unaffected sites if pine and camphor tree species were present (Fig. 1). For reliably extracting growth patterns of the tree stands, the sample plots were established at the closest distance to the tunnels (~40-500 m) and the farthest distance from the springs and surface waters (Fig. 1). Meanwhile, topographic and hydrological conditions on all the selected sample plots were almost the same. Two increment cores were prepared during October 2017

and September 2018—at ~1.3 m of breast height using a 5.144-mm increment borer from different directions—from healthy mature individuals for both tree stands across the sample plots in the study site. The number of the sampled individuals within the affected site were equal to 69 (36 and 33 individuals across the karst and non-karst plots, respectively) and 54 (27 individuals across both karst and non-karst plots) for the pine and camphor stands, respectively. In contrast, within the unaffected site, they were equal to 60 (30 individuals across both karst and non-karst plots) and 48 (24 individuals across both karst and non-karst plots) for the above-mentioned stands, respectively. All core samples were air-dried and mounted onto the grooved boards. Then, they were sanded using up to P1000 (ISO/FEPA Grit designation) sandpaper until the annual ring boundaries were clearly visible for each core. The prepared cores were cross-dated to find possible missing or false rings and to obtain a true calendar year using a skeleton-plot method under the microscope (Stokes and Smiley, 1996). Further, we followed the procedure described in the protocol suggested by Grissino-Mayer (2001), providing step-by-step directions within the COFECHA to ensure that a missing ring has been placed correctly during cross-dating. Afterward, ring widths were measured to the nearest 0.001 mm using a Velmex tree-ring measurement system (Velmex Inc.) (Wang et al., 2019). The accuracy of measurements was investigated by COFECHA (Grissino-Mayer, 2001; Holmes, 2001). Tables S2 and S3 present a summary of the descriptive statistics (COFECHA output) for tree-ring width chronologies (of individual trees) of the pine and camphor stands, respectively, across all the karst and non-karst plots (areas) within the affected and unaffected sites. As shown in these tables, the ring-width series from both tree stands produced highly significant mean correlations across all plots, indicating that the cross-dating (between their individual trees) was performed correctly and with high accuracy. When cross-dating, in order to achieve trustable results, the "autocorrelation" or "carryover" of ring width observations was removed through statistical prewhitening (Cook, 1985).

Long-term interactions between the tree and its water sources can be captured by a series of widths of annual growth rings in the tree (Ferguson and George, 2003; Zweifel et al., 2006; Perez-Valdivia and Sauchyn, 2011; Creutzfeldt et al., 2015; Berdanier and Clark, 2018). Due to weaker dependence on tree age, the BAI series—calculated according to Jump et al. (2006) as $BAI = \pi (R_n^2 - R_{n-1}^2)$, where R and n correspond to the tree radius and date of tree-ring formation for an individual tree, respectively—were used instead of the ring-width series to get more accurate and reliable information regarding the growth dynamics of the tree stands and their water sources (Schuster and Oberhuber, 2013; Obojes et al., 2018). In a healthy tree, during the mature phase, BAI may have an increasing (positive) (Phipps and Whiton, 1988; Fekedulegn et al., 2003) or stabilizing trend (LeBlanc et al., 1992), but it will not show a declining (negative) trend until the tree begins to senesce (Duchesne et al., 2003; Peñuelas et al., 2008). Thus, a negative BAI pulse, which may occur under various stresses, such as water stresses resulting from climatic (Pedersen, 1998; Phillips et al., 2010; Levesque et al., 2013; Barbeta et al., 2015) and/or non-climatic perturbations (Bogino and Jobbágy, 2011; Zheng et al., 2017) can be considered a solid indicator of a true decline in tree growth (in response to any stress-driven event) (Muzika et al., 2004; Peñuelas et al., 2008; Obojes et al., 2018; Wang et al., 2019). Accordingly, a plot-by-plot analysis was conducted using the BAI series of the tree stands across different (karst and non-karst) landscapes at the affected and unaffected sites to track negative growth pulses linked to TIGD of individual tunneling events for each tree stand when the stand BAI level shifted from a positive to a negative trend during each event (Fig. 5a-c). For developing the stand-scale BAI chronology, unstandardized annual BAI series were averaged over all mature individual trees across each plot as described by Rodríguez-Catón et al. (2015). For adding a long-term perspective, multi-year average mature BAI chronologies were also developed to track and extract negative growth trends linked to TIGD of individual tunneling events within the stand and landscape scales over four different time intervals after each event; the first three-time periods included the beginning of the chronology (mature phase) to the end of the construction period of each tunnel, while the last time period included the entire chronology period from beginning to end (Fig. 7). For quantifying the extent of (individual trees) growth responsiveness to TIGD of individual tunneling events, a plot-by-plot analysis was performed to extract the dropped BAI values due to TIGD during each event (that is, from a short-term perspective) within the stand and landscape scales (Fig. 6a,b). Given the mediating effects of climate, which positively or negatively influenced the growth level of the stands (see Results), the quantifications were made based on relative estimates of effect sizes. This meant that for the stands across the affected plots, the dropped BAI values linked to TIGD during each tunneling event were incorporated together with the increased and dropped BAI values associated with simultaneous climate events. Since no effect of tunneling was observed in the unaffected plots (see Results), only the increased and dropped BAI values linked to the climate events were incorporated together across these plots during each tunneling event, allowing for differentiation between the effects of tunneling with and without mediating effects of climate. Additionally, to evaluate the aggregated negative effects of all three tunneling events on the growth level of the stand from a long-term perspective, a plot-by-plot comparison was made using unstandardized annual average mature BAI values (of individual trees) of the stand across each affected (karst or non-karst) plot and its comparable unaffected plot. This procedure allowed first to quantify the annual average dropped growth level and then quantify the overall average dropped growth level (concerning TIGD of all three tunneling events) for each stand across each affected plot when comparable sample sizes were considered for all mature BAI chronologies (for example, 1991–2018 and 1994–2018, respectively for the pine and camphor stands across the tunnel 1 karst plot, 1999–2017 for both stands across the tunnel 3 karst plot; Fig. 8a-c). In fact, BAI values for a given tree stand in a given plot within the unaffected site were considered as the reference for comparison. Accordingly, and considering the mediating effects of climate, our results were reported as relative estimates of effect sizes.

Although unstandardized average mature BAI chronologies might have been tricky for extracting non-climatic signals of TIGD that we were primarily interested in, they could not be effective for tracking common climate signals (as reported by Cook et al. (1995) and Jump et al. (2006)). Therefore, a standardization procedure was used to homogenize the variance of unstandardized BAI series to allow their direct comparison (Cook, 1985; Cook and Briffa, 1990). In fact, this procedure could help to maximize common climatic signals (Briffa et al., 1996; Helama et al., 2004) and to better differentiate climate-caused growth pulses from tunneling-induced growth pulses within the stand and landscape scales. Our analysis focused on BAI trends during the mature phase of growth (Fig. 2a,b). The climate variables' 30-year continuous records (1988–2018) were collected from the local weather station established in an open place within the study site, 10–55 m higher than the sample plots (Fig. 1). The considered climate variables were total annual and seasonal (growing season; May–September) rainfall and average annual and seasonal temperature. Besides, a response function analysis method (Biondi and Waikul, 2004; Wang et al., 2019) was applied for plot-by-plot testing of the relationships between climate variables and annual average mature BAI of individual trees within the stand and landscape scales at the affected and unaffected sites (Fig. S1). For this analysis, annual total rainfall and average temperature were considered from October of the previous year to September of the current year. In this procedure, linking growth to climate could be excluded in months after growth cessation (Jump et al., 2006; Peñuelas et al., 2008). Additionally, using monthly rainfall series of the 30-year base period (1988–2018) in the study site, three different climate indices, including rainfall anomaly index (RAI), standardized precipitation index (SPI), and decile method (DM), were calculated on an annual basis. This allowed us to identify and determine the type (wet and drought), duration, and intensity of climate events (Dogan et al., 2012; Lima et al., 2019) that occurred in the study site. Given that the numerical results of the different climate indices were primarily challenging to analyze, an overall classification of the indices was used to evaluate the degree of intensity of wet and drought events within the base period under consideration (Fig. 3). It was based on the

classification proposed in a previous study (Dogan et al., 2012). After identifying the climate events, a plot-by-plot analysis was performed to quantitatively estimate the extent of (individual trees) growth responsiveness to individual climate events in a short-term perspective within the stand and landscape scales at the affected and unaffected sites. This was accomplished by incorporating the increased or dropped BAI values linked to each event (Fig. 4a,b).

The statistical analyses were carried out using IBM SPSS Statistics 25 (IBM Co., NY, USA).

## 3. Results

### 3.1. Tracking relationships between climate and growth

A response function analysis indicated that mature BAI was highly sensitive to rainfall and temperature for the pine and camphor stands across all the affected and unaffected plots (Fig. S1a,b). As shown in Fig. S1a,b, annual total rainfall, and total rainfall in the growing season had a strongly positive effect on the growth level of both stands across all the

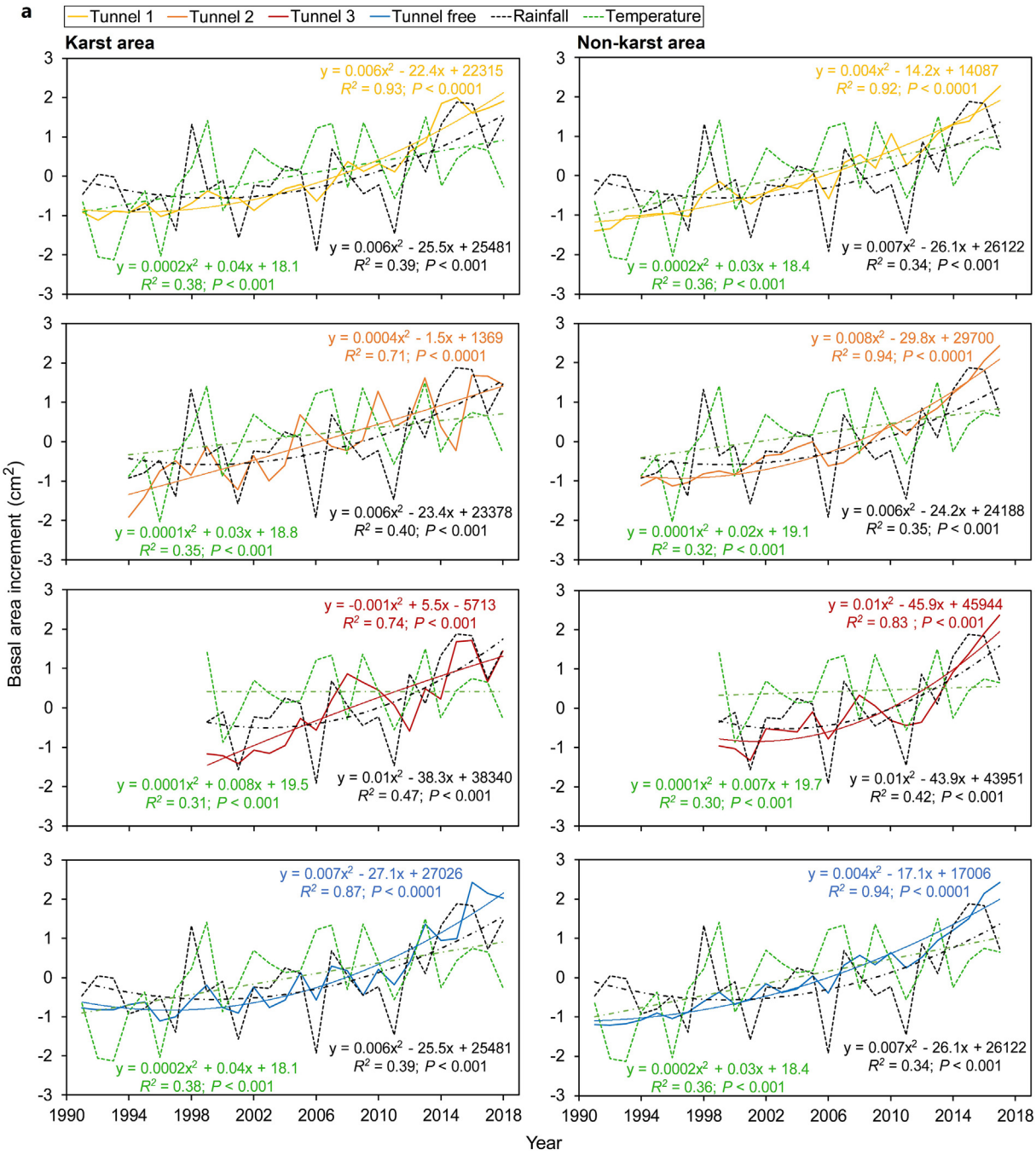


**Fig. 2.** Relationships between climate and growth over time. A plot-by-plot analysis was performed to extract relationships between standardized annual climate variables (annual total rainfall and average temperature; based on a 12-month period beginning with October of the previous year) and standardized annual average mature BAI of the pine (a), and camphor (b) stands across the karst (left columns) and non-karst (right columns) areas within the affected (the first three rows) and unaffected (the last row) sites. The colored dashed lines represent significant trends with corresponding equations, correlation coefficients (R), and statistical significance (P).

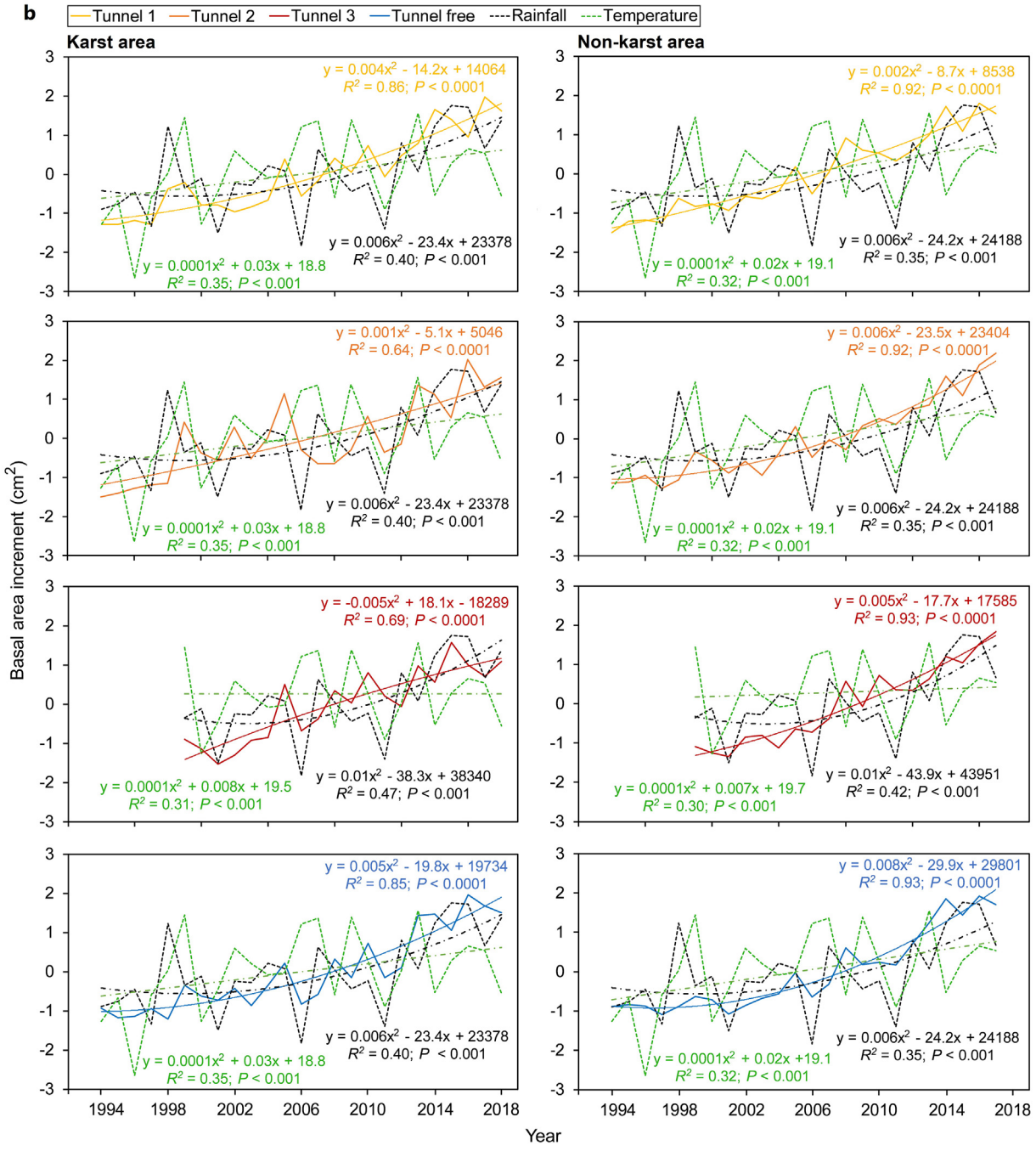


**Fig. 2** (*continued*).

plots (*P*-value for both stands across most of the plots was less than or equal to 0.001, Tables S4 and S5). A similar but weaker response was also found for annual average temperature, and average temperature in the growing season for both stands across most of the plots (*P*-value for both stands across most of the plots was less than 0.05, Tables S4 and S5).

The study area presents the unstandardized annual total rainfall and average temperature during 30 years (1988–2018) in Fig. S2. There was a strong increasing trend in rainfall with a sharp change (decrease) in slope after 2006 ($R^2 = 0.43$, $P < 0.001$) as well as a visible warming trend in temperature ($R^2 = 0.40$, $P < 0.001$) throughout the studied period. The relationships between standardized annual climate variables and standardized annual mature BAI over time are shown for both pine and camphor stands across each plot in Fig. 2a,b, respectively. Our observations showed that both stands' high and low BAI values across all the plots often coincided with extremes of rainfall and temperature or experienced a one-year lag behind them. This lag effect reveals that in addition to the current year climate, the previous year climate might have also been a strong effect on the growth level of the stands in the current year (Jump et al., 2006; Peñuelas et al., 2008; Millar et al., 2012). As shown in Tables S4 and S5, there was a highly significant positive correlation between the BAI series of both stands with the previous year total rainfall (*P*-value for both stands across all the plots was less than or equal to 0.001) and a relatively significant positive correlation between them with the previous year average temperature (*P*-value for both stands across most of the plots was less than 0.05). This could greatly clarify the current-year ring width variability associated with the previous year climate. Further, it could also be explained by a significant autocorrelation in the tree-ring width series as observed in both stands across all the plots (autocorrelation values varied between 0.366 and 0.553 ($P < 0.001$) for the pine stands and between 0.411 and 0.692 ($P < 0.001$) for the camphor stands across all the karst and non-

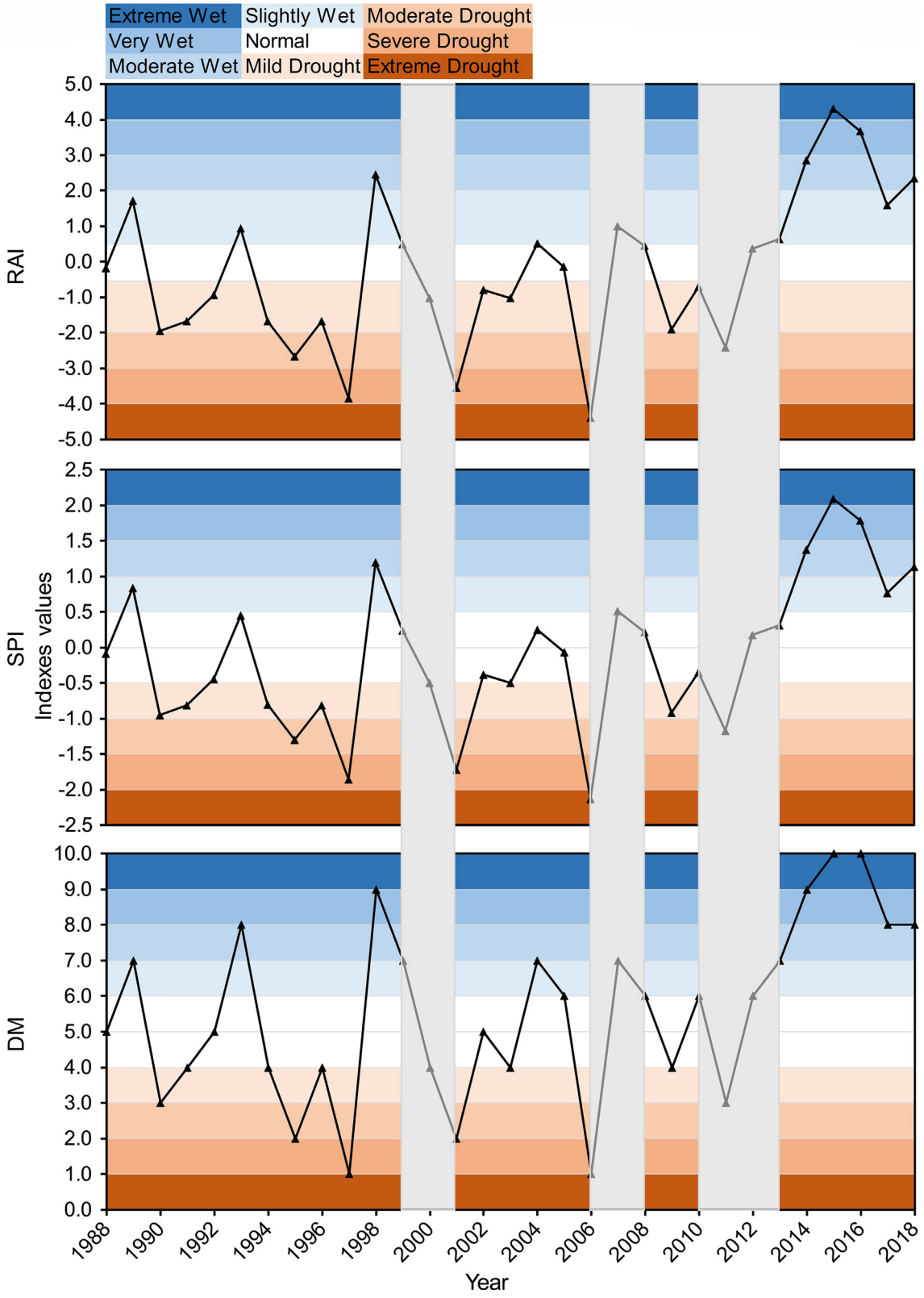


**Fig. 3.** Type, duration, and intensity of climate events based on RAI, SPI, and DM indices at the study site. The climate indices were calculated using monthly rainfall series for a 30-year base period (1988–2018) in the region. Each climate event's degree of intensity was determined based on the global classification (Lima et al., 2019). The shaded areas represent periods of tunnel construction on the study site (1991–2001, 2006–2008, and 2010–2013).

karst plots (areas) within the affected and unaffected sites, Tables S2 and S3). This was in line with previous studies (Breitenmoser et al., 2014; Barichivich et al., 2021), which used the autocorrelation observations of tree-ring width series to assess and extract the significance of the previous year climate. They showed that the previous year climate could explain up to 30% of current-year tree growth dynamics. Besides, our observations showed an increasing trend in the standardized BAI of the stands across all the plots during 2007–2018, which was very similar to the observed

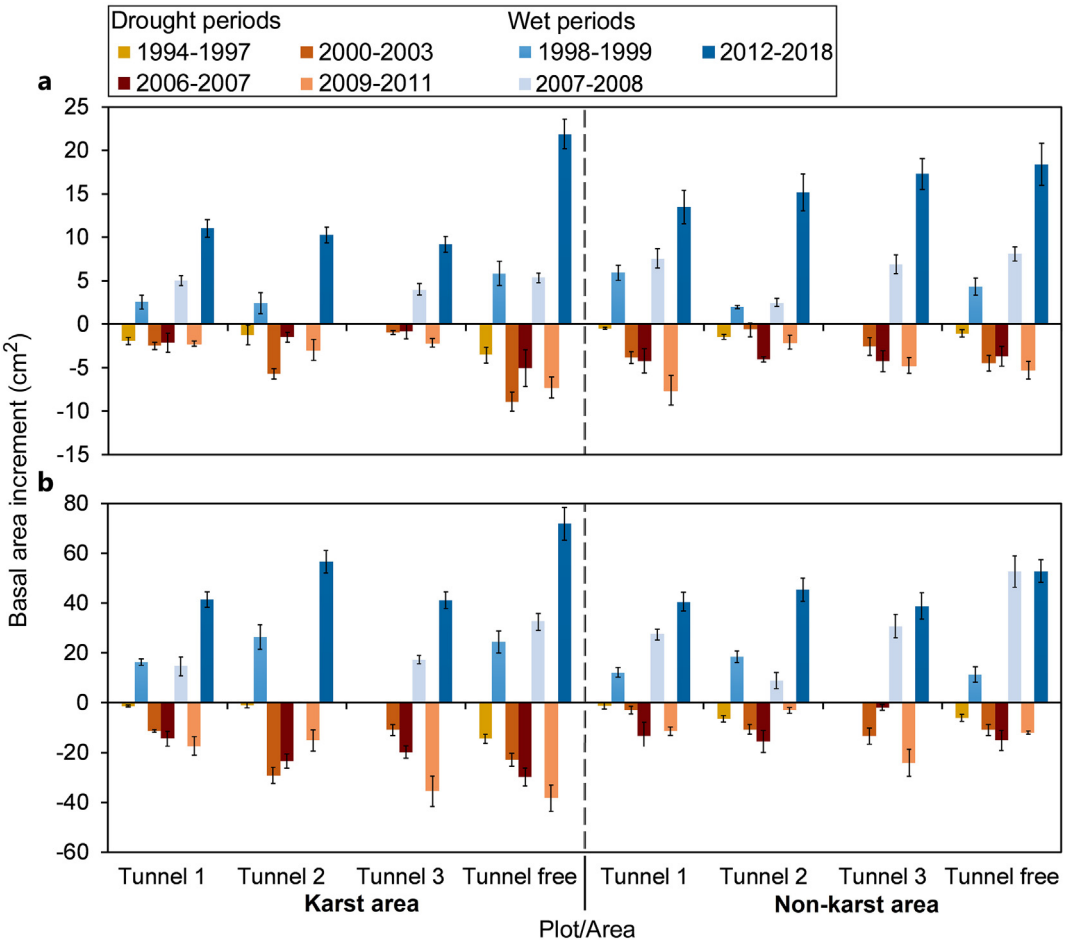


**Fig. 4.** Short-term responsiveness of growth to the climate variability of individual events. Using unstandardized annual average mature BAI values (of individual trees) of the stand, a plot-by-plot analysis was performed to extract the degree of short-term responsiveness of growth to individual climate events for the pine (a), and camphor (b) stands across the karst and non-karst areas within the affected and unaffected sites. The degree of the effect associated with each climate event is presented as the total mean ± SE of mean (dropped or increased) BAI values of individual trees within the stand/landscape scale. The dropped BAI values linked to the tunneling events were excluded across the affected plots.

increasing trend in rainfall than in temperature (Fig. 2a,b). Recent (2012–2018) standardized BAI peaks were largely converged toward standardized rainfall peaks—just when rainfall extremes had taken place—across all the plots or were soared above them across some of the plots (for example, see temporal trends in standardized BAI and rainfall for both stands across tunnel 1 and tunnel-free karst and non-karst plots shown in Fig. 2a,b). As explained above, this highlights the stronger effect of rainfall on the growth level of the tree stands than temperature.

### 3.2. Growth responsiveness to climate variability

According to the three different climate indices (RAI, SPI, and DM; see Materials and Methods for details), several cycles of drought and wet were observed for the study area over the analyzed chronologies (1990–2018; Fig. 3). Through plot-by-plot comparisons of growth trends —using standardized BAI series—of the stands (Fig. 2a,b) with climate trends associated with drought or wet events (Fig. 3), we found that the growth trends of the stands across all the plots closely tracked climate trends during each drought or wet event. So that, both stands across all the (either affected or unaffected) plots primarily showed a declining (or negative) BAI pulse during drought events or, conversely, an increasing (or positive) BAI pulse during wet events. Negative and positive BAI pulses might have been the signals for reducing and increasing stand water uptake over drought and wet events, respectively (Anderegg and Anderegg, 2012; Barbeta et al., 2015; Creutzfeldt et al., 2015; Gao et al., 2018). As shown in Fig. 4a,b, the degree of growth responsiveness to individual climate events has varied for each stand across each of the plots within both affected and unaffected sites. For instance, during the 2006 drought, which was the shortest period but was the most severe level of drought experienced over the analyzed period, the BAI values of the stands across all the plots were sharply negative and approximately close to the dropped BAI values for longer droughts with 3-year and 4-year durability periods (that is, 2000–2003 and 2009–2011 droughts, respectively). The highest and lowest dropped BAI values associated with this drought were −51 and −8 mm for the pine stands across the tunnel-free and tunnel 3 karst plots, respectively, and −297 and −21 mm for the camphor stands across the tunnel-free karst plot and the tunnel 3 non-karst plot, respectively (Fig. 4a,b). Growth responses to wet events were also as strong as, or even stronger than, those to drought events. For instance, between 2012 and 2018, the beginning of which approximately coincided with the completion of the third (last) tunnel (2010 − 2013), the study area experienced an exceptional and unprecedented wet period (average annual total rainfall increased by about 26.7 mm during this six-year climate period; Fig. S2), which remarkably influenced the growth level of the stands across all the plots. The highest and lowest increased BAI values associated with this event were 218 and 92 mm for the pine stands across the tunnel-free and tunnel 3 karst plots, respectively, and 719 and 386 mm for the camphor stands across the tunnel-free karst plot and the tunnel 3 non-karst plot, respectively (Fig. 4a,b). Overall, as also illustrated in the above examples, the camphor stands and karst plots at both affected and unaffected sites showed

the strongest growth pulses during all the climate events within the stand and landscape scales, respectively (Fig. 4a,b). Different feedback among the stands might have been primarily related to the genetic differences in their growth conditions (as mentioned earlier) (Mohan et al., 2004; Bradley and Pregitzer, 2007; Bowman et al., 2013) or their different water-use strategies (for example, rooting depth, stomatal control) (Ehleringer and Dawson, 1992; Lloyd, 1997; Lin et al., 2015; Fan et al., 2017). While, different feedbacks among the landscapes could be largely explained by the high heterogeneity of water flow dynamics (within plant-available water-source pools) in the karst landscapes compared to the non-karst landscapes (Ford and Williams, 2007; Bonacci et al., 2009). In fact, it forces plants living in the karst landscapes to be far more sensitive (or vulnerable) to any water fluctuation and stress than plants living in the non-karst landscapes (Liu et al., 2019; Lv et al., 2020; Wu et al., 2021).

### 3.3. Tracking indicator pulses of growth linked to TIGD

Through plot-by-plot comparisons of unstandardized average mature BAI chronologies of the stands within the affected site with those within the unaffected site (Fig. 5), we tracked growth pulses linked to TIGD during each tunneling event to disentangle them from growth pulses mediated by climate events. During the establishment of tunnel 1 (1999–2001), which also coincided with a long-term drought (2000 − 2003), there was a sharp (reduction) interruption in the BAI trend of both stands across all the (either karst or non-karst) plots within the affected site (Fig. 5a-d). Moreover, a similar trend was also observed for the stands across comparable plots within the unaffected site. After the completion of the tunnel construction in 2001, as the severity of the drought decreased, the growth level of both stands increased across all the affected and unaffected plots except for the tunnel 1 karst plots. Negative BAI pulses observed for the pine and camphor stands across the tunnel 1 karst plots returned to a positive trend in 2003 and 2004, respectively (Fig. 5a,c). A relative estimate of the tunneling effects on the short-term growth level of the tree stands across the affected and unaffected plots during the establishment of tunnel 1 (Fig. 6a,b) showed that the growth level of the stands was significantly negative within the site of tunnel 1, not only in the karst plots but also in the non-karst plots. In contrast, the growth level of the stands was significantly positive at all the tunnels 2 and 3 and tunnel-free karst and non-karst plots. These negative BAI pulses tracked in the tunnel 1 karst and non-karst plots, which were clearly distinguishable from (climate-mediated) positive BAI pulses observed in most of the other plots, will most likely represent TIGD (Zheng et al., 2017) in relation to the construction of tunnel 1. During the establishment of tunnel 2 (2006–2008), negative BAI pulses linked to TIGD were only observable at the tunnel 2 karst plots for both stands (Figs. 5a,c and 6a,b). In the tunnel 2 non-karst plots as well as the other karst and non-karst plots within the construction sites of tunnels 1 and 3, the stands not only showed no negative BAI pulse linked to TIGD but also displayed a positive BAI pulse associated with a wet event in 2007 and 2008 (Figs. 4a,b, 5a-d and 6a,b). A similar climate-related pulse signal was also observed for both stands across the tunnel-free karst and non-karst plots. One year after the completion of the tunnel construction (that is, in 2009), negative BAI pulses returned to a positive trend for both stands across the tunnel 2 karst plots (Fig. 5a,c).

During the establishment of tunnel 3 (2010–2013), negative BAI pulses linked to TIGD were observable for both stands across both tunnel 3 karst and non-karst plots (Figs. 5a-d and 6a,b). The degree of growth responsiveness to this tunneling event was more pronounced between 2010 and 2012. Because, from 2012 onwards, simultaneously with the beginning of the most extreme wet period (2012–2018), the BAI level of the stands across the affected plots was significantly promoted and switched (from a negative) to a positive trend. The BAI level of the stands across all the other plots was significantly decreased or negative in 2010 and 2011 associated with a drought event (2009–2011) and was remarkably increased or positive between 2012 and 2018 associated with the mentioned wet event (Figs. 4a,b and 5a-d). It is worth noting that, besides the positive and strong mediating effects of wet climate events, another important reason for promoting and recovering the growth level of the stands across the affected plots might have been related to control measures for tunnel establishment, such as grouting and sealing (Zheng et al., 2017) because it could potentially minimize groundwater leakage into tunnels (Lv et al., 2020).

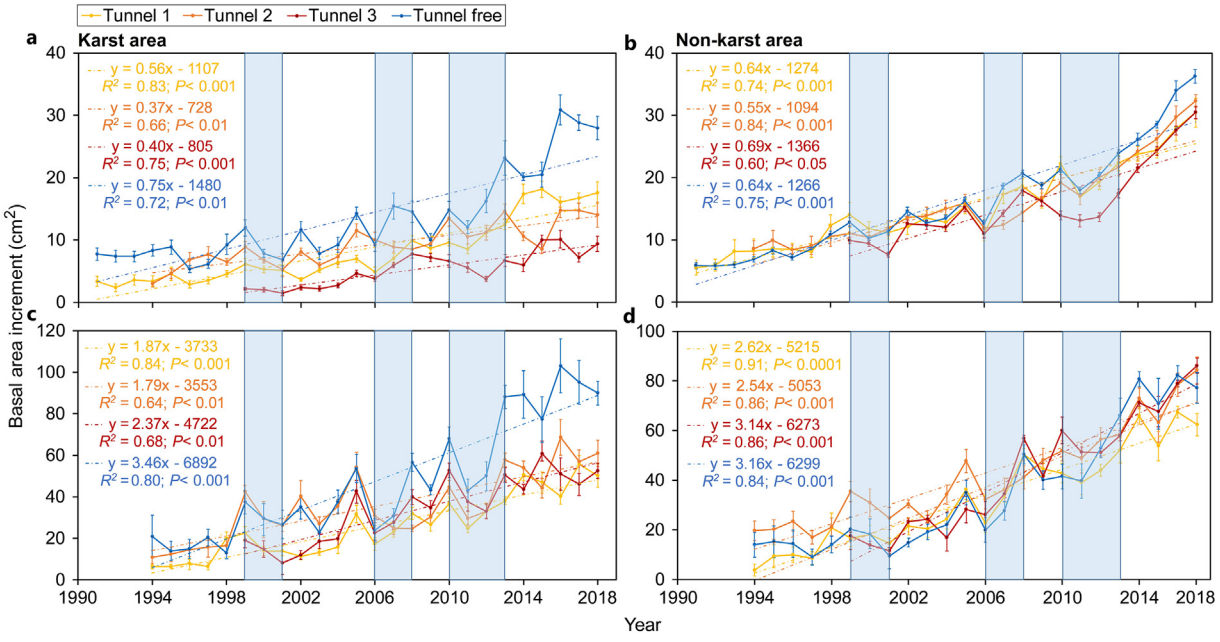


**Fig. 5.** Short-term growth pulses linked to TIGD of individual tunneling events. Using unstandardized annual average mature BAI (of individual trees) of the stand, a plot-by-plot analysis was performed to track and extract negative growth pulses linked to TIGD of individual tunneling events over short-term intervals (that is, during each event) for the pine (a, b), and camphor (c, d) stands across the karst (a, c), and non-karst (b, d) areas within the affected and unaffected sites. All results are represented as mean ± SE of BAI values of individual trees within the stand/landscape scale. The colored dashed lines represent significant trends with corresponding equations, correlation coefficients (R), and statistical significance (P). The shaded areas represent periods of tunnel construction in the study site (that is, 1991–2001, 2006–2008, and 2010–2013).

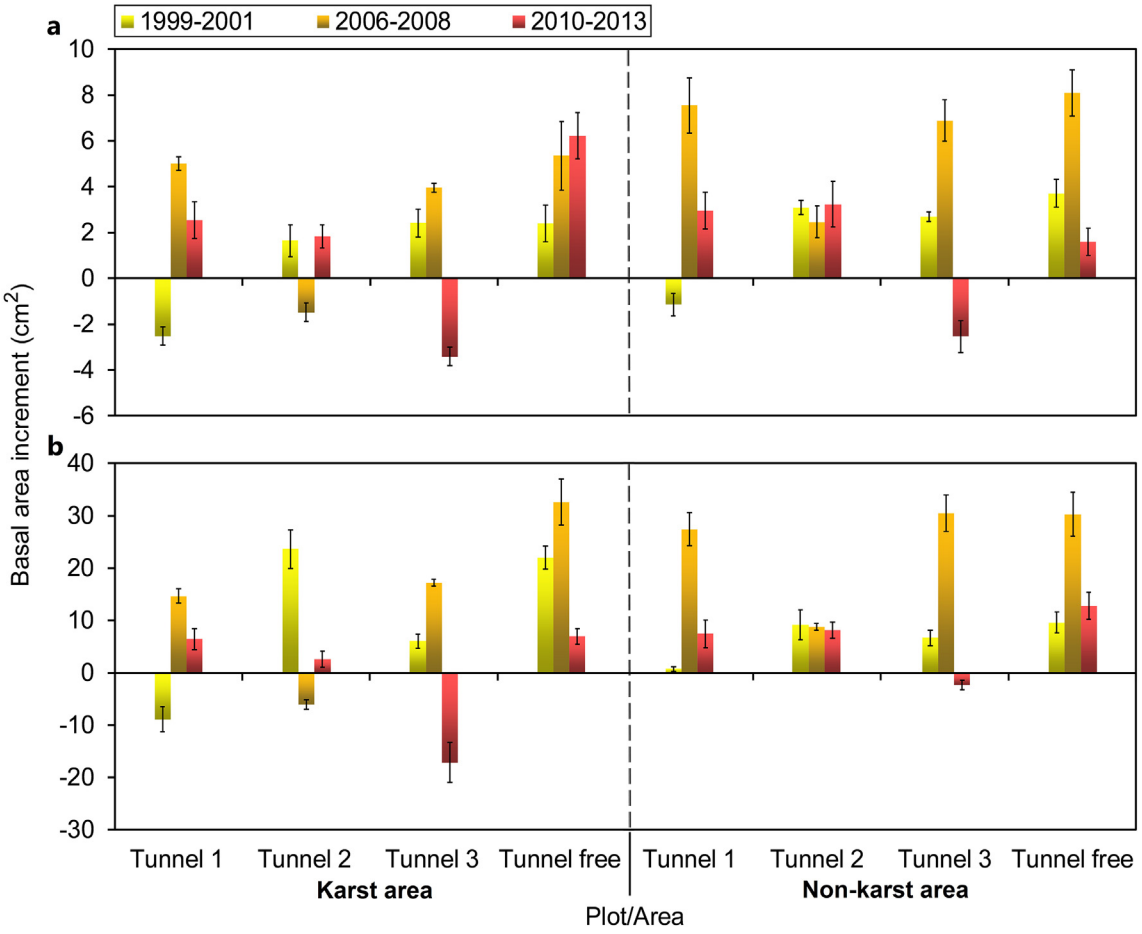


**Fig. 6.** Short-term responsiveness of growth to TIGD of individual tunneling events. Using unstandardized annual average mature BAI values of the stand, a plot-by-plot analysis was performed to extract the degree of short-term responsiveness of growth to TIGD of individual tunneling events for the pine (a), and camphor (b) stands across the karst and non-karst areas within the affected and unaffected sites. The degree of the effect associated with each tunneling event is presented as the total mean ± SE of the mean (tunneling-induced) dropped BAI values of individual trees within the stand/landscape scale. Due to the climate's positive or negative mediating effects, the results were reported as relative estimates of effect sizes (see Materials and Methods for details).

### *3.4. Growth responsiveness to TIGD-linked hydrological variability*

Although the effects of TIGD of individual tunneling events on short-term growth dynamics of the stands were tracked only at the (karst and non-karst) areas designated for construction of each tunnel, no negative pulse of growth as an indicator pulse linked to TIGD was observed for the stands across all the other plots within the affected site over short time intervals. This could be possibly due to the pervasive and strong mediating effects of climate events, especially droughts. Therefore, a multi-year average method was used to visualize better possible undetected growth pulses associated with TIGD over longer time intervals (see Materials and Methods for details). As shown in Fig. 7, over four different time intervals, particularly the last (longest) period, the multi-year average mature BAI slope of the stands across all the affected plots, especially at the karst plots (Fig. 7a,c), was significantly lower than those across the unaffected plots. This was a masked long-term (negative growth pulse) signal due to the aggregated effects of TIGD in relation to the establishment of all three tunnels. Moreover, it suggested that the possibility of promotion and restoration to the normal growth level—like what has been observed for the stands across the unaffected areas over the entire chronology period—might have been weakened considerably for both tree stands across all the affected areas, maybe forever.

For plot-by-plot estimating the aggregated long-term negative effects of all three tunneling events, comparable sample sizes were considered for mature BAI chronology of the stand across each (karst or non-karst) plot within the affected site and its corresponding plot within the unaffected site (see Materials and Methods and Fig. 8a,b for further details). As shown in Fig. 8a,b, the annual average growth level of the stands (AAGLS) across all the affected karst plots was significantly less than those across corresponding karst plots within the unaffected site. The overall average dropped growth level of the stands across the tunnels 1, 2, and 3 karst plots over the analyzed chronologies were equal to −62, −56, and −104 mm for the pine stand and were equal to −216, −120, and −181 mm for the camphor stand, respectively (Fig. 8c). This illustrated that both stands across all the affected karst plots were significantly vulnerable to TIGD. However, the camphor stands showed considerably more vulnerability than the pine stands, possibly for the same reason mentioned earlier (genetic variations in growth conditions and different water-use strategies among the stands). At most of the affected non-karst plots, decreases in AAGLS—especially for the camphor stands—were not as significant as those across the affected karst plots. This indicated that the stands across the affected karst landscapes were much more vulnerable (to TIGD) than those across the affected non-karst landscapes, possibly for the same reason mentioned earlier (higher rate of water circulation and drainage within the karst landscapes). The overall average dropped growth level of the stands were equal to −9, −12, and −38 mm for the pine stands across the tunnels 1, 2, and 3 non-karst plots, respectively, and was equal to −30 mm for the camphor stand across the tunnel 1 non-karst plot (Fig. 8c). The camphor stands across the tunnels 2, and 3 non-karst plots not only showed no negative AAGL but also had a

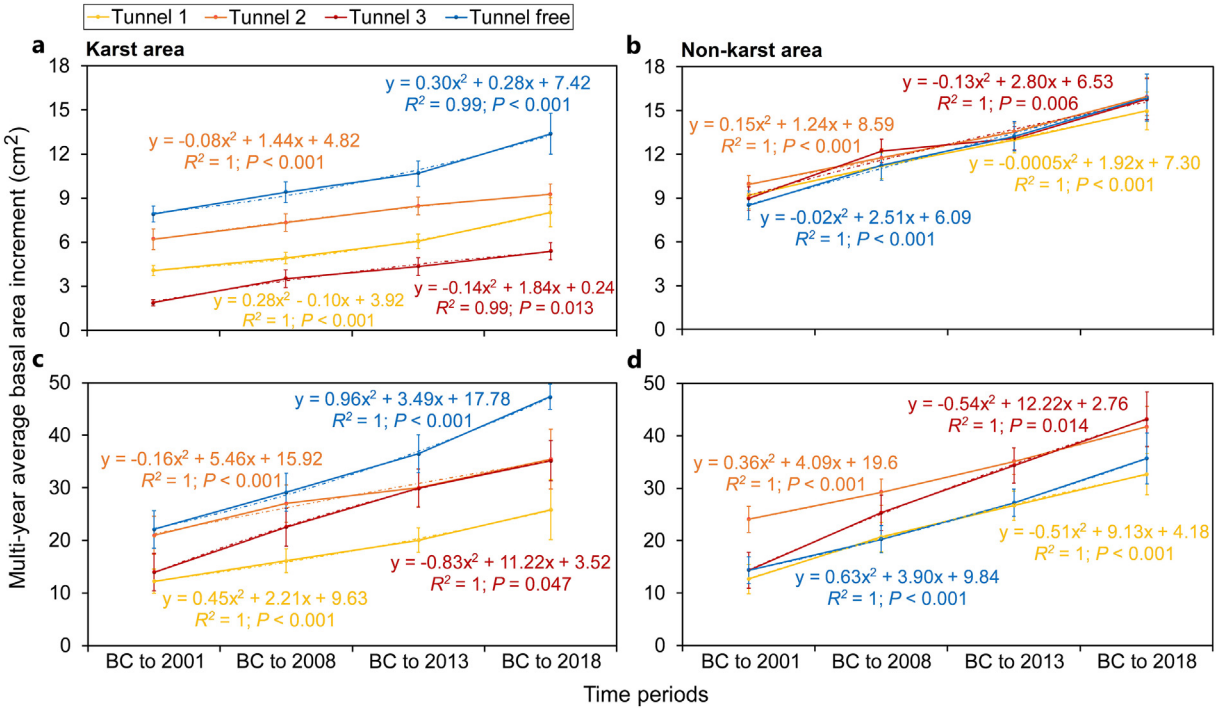


**Fig. 7.** Long-term growth pulses linked to TIGD of individual tunneling events. Using multi-year average mature BAI of the stand, a plot-by-plot analysis was performed to track and extract negative growth trends linked to TIGD of individual tunneling events for the pine (a, b), and camphor (c, d) stands across the karst (a, c), and non-karst (b, d) areas within the affected and unaffected sites over four long-term intervals after each event; the first three-time periods included the beginning of the chronology (BC; during the mature phase) to the end of the construction period of each tunnel (that is, 2001, 2008, and 2013), while the last period included the entire chronology from beginning to the end (BC to 2018). A lower slope for the stand across each affected plot than its comparable unaffected plot (as observed for the tree stands across most of the affected plots, especially across the karst plots) suggested that the stand might have been responsive to TIGD. The error bars represent means ± SEs of mean BAI values of individual trees within the stand/landscape scale. The colored dashed lines represent significant trends with corresponding equations, correlation coefficients (R), and statistical significance (P).

significant positive AAGL, as the overall average increased growth level of the stands were equal to 60 and 14 mm across the tunnels 2 and 3 non-karst plots, respectively (Fig. 8c).

## 4. Discussion

In this study, stand- and landscape-scale observations of short- and long-term plant-water interactions were presented during and after establishing three tunnels via tracking negative growth pulses induced by a single or a collection of tunneling events. Our findings showed that tunneling-induced growth pulses (TIGPs) were recognizable and common pulses for both stands across most of the affected areas of the landscapes, even when they were strongly mediated by drought and wet climate extremes. Observing such pulses could be a signal of a decrease in stand water uptake due to TIGD in the affected areas. While the negative feedback from tunneling was stronger and more prevalent across the camphor stands and karst landscapes, the same feedback also existed, albeit at weaker degrees, across the pine stands and non-karst landscapes. Although TIGPs often overlapped with drought-induced growth pulses (DIGPs), they were still distinguishable from each other. Our short-term observations showed that TIGPs, like DIGPs, in most of the affected areas, appeared to be recovering (or promoting in response to each wet event) as much as the normal growth levels observed for the stands across the unaffected areas (Figs. 5a-d and 6a,b). However, our long-term observational evidence revealed that they (unlike DIGPs) were never fully recovered (Fig. 7a-d); because the overall average growth level of the stands in most of the affected areas was still remarkably negative (Fig. 8c) even with the mediation of extremely favorable climate conditions (that is, the very wet six-year climate period (2012–2018) after the construction of the final (third) tunnel in 2010–2013). This clearly indicates that the magnitude of ecohydrological vulnerability to tunneling-induced water stress has been far more severe than drought-induced water stress. It is also suggested that even this might have been somewhat irreversible for the following reasons. First, as shown in this study, DIGPs were rapidly and strongly promoted in response to favorable climate conditions or even reduction in drought intensity. In contrast, TIGPs, although significantly, but belatedly (with a time lag) were promoted in response to them. This could be because, unlike tunneling, droughts could not deplete all the water storage of plant-available water-source pools (especially groundwater) instantly and dramatically (see conceptual model shown in Fig. 9). Second, our observations in previous work showed that due to tunneling, at the beginning of the first tunnel construction (1999–2001), a significant portion of groundwater storage, particularly in the upper zones (within the unsaturated zone) where a larger fraction of root biomass occurs, has been out of plant access for a very long period, or maybe forever (Liu et al., 2019). Besides, as documented in the previous work, even soil water content in superficial soil layers (0–40 cm) was significantly reduced in the tunnel-affected areas. This has led to a remarkable reduction in soil water uptake by the studied tree species (Liu et al., 2019), possibly due to approaching the moisture level of the soil layers to a (tunneling-induced) threshold or wilting point for plant use (Feldman et al., 2018; Gokdemir et al., 2019). To better understand the effects of tunneling and drought on tree growth dynamics, a conceptual model is presented in Fig. 9.

Overall, our findings show that the tree's annual growth rings can serve as a very efficient and cost-effective technique for monitoring the growth conditions of forest stands in response to any water stress resulting from the individual (climate-mediated) anthropogenic events. This may be principally because all the key information needed to develop a probabilistic model with interactions between forest stands, water resources, and climate and anthropogenic disturbances at various spatial-temporal

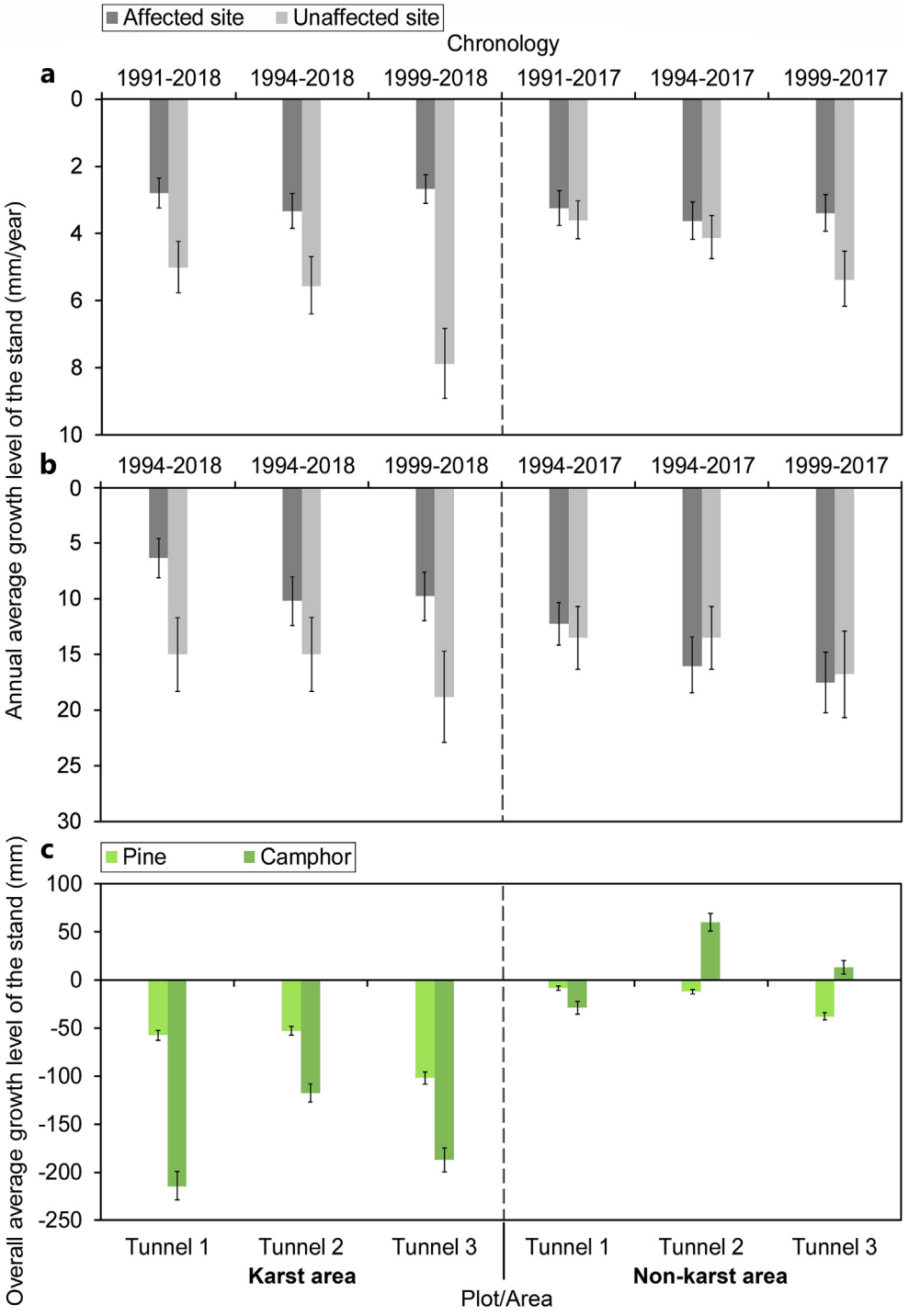


**Fig. 8.** Long-term responsiveness of growth to TIGD of a collection of tunneling events. Using unstandardized annual average mature BAI values of the stand, a plot-by-plot comparison was performed to quantify the annual average dropped growth level (due to TIGD of all three tunneling events) for the pine (a), and camphor (b) stands and the overall average dropped growth level (or aggregated average negative growth level for the same reason) for both stands (c) across the karst and non-karst areas within the affected site. For a given tree stand in a given (karst or non-karst) plot within the affected site, there was a comparable model within the unaffected site. It allowed comparison of growth levels (or BAI values) within the stand and landscape scales when comparable sample sizes were considered for all BAI chronologies (for example, 1991–2018 and 1994–2018, respectively, for the pine and camphor stands across the tunnel 1 karst plot, 1999–2017 for both stands across the tunnel 3 karst plot). Accordingly, and considering the mediating effects of climate, the results were reported as relative estimates of effect sizes. The error bars represent means ± SEs of mean BAI values of individual trees within the stand/landscape scale.

scales may be already and simultaneously incorporated (or recorded) into the annual growth rings of trees (Biondi and Strachan, 2012). Thus, they can represent a realistic model of the function of the forest ecosystem under various climate and hydrological variability (Loaiciga et al., 1993).

## 5. Conclusions

Analysis of the annual growth rings of two dominant drought-tolerant tree stands living in different (karst and non-karst) landscapes in a mountainous forest ecosystem across the southwest of China provided clear

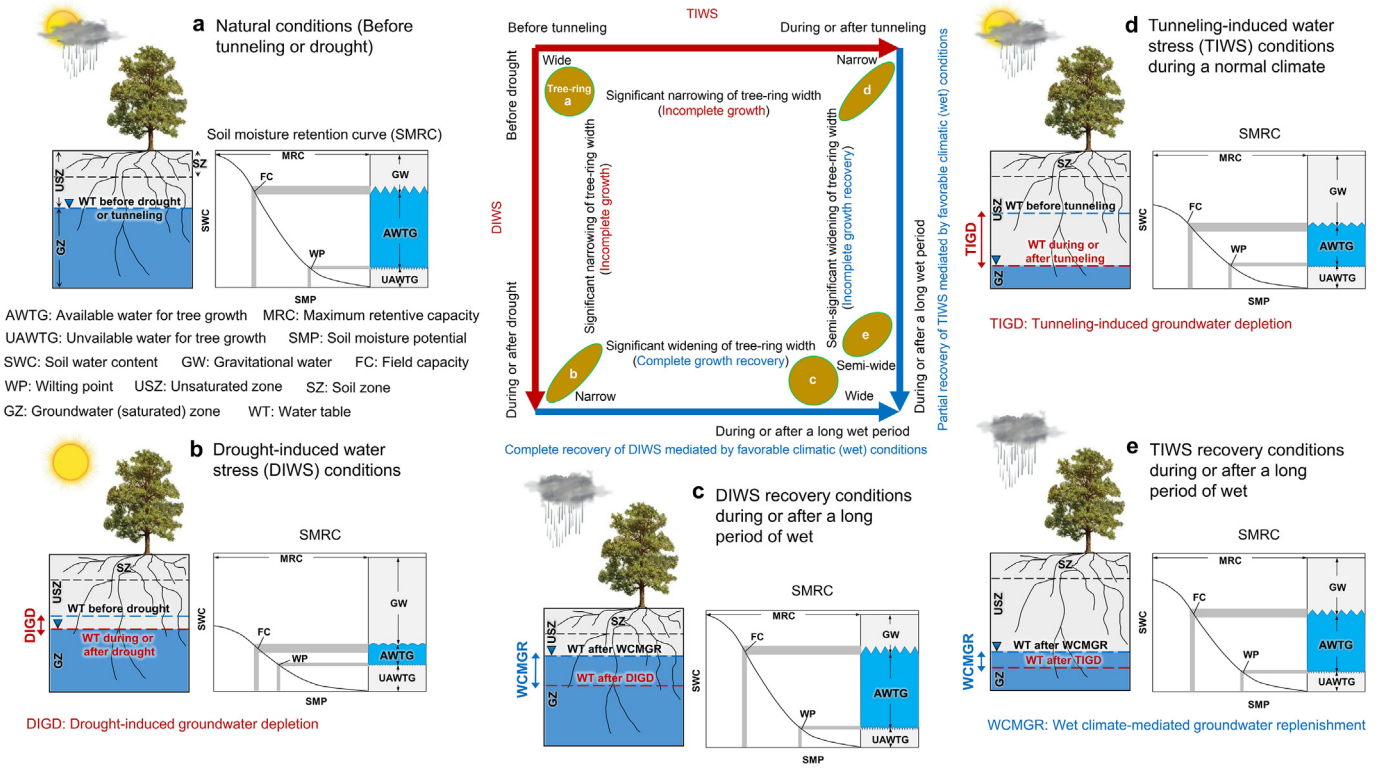


**Fig. 9.** Conceptual model regarding shifts in tree growth responses under conditions without and with water stress. A, shows natural or lack of water stress conditions (before tunneling or drought) during a normal climate. Under these conditions, sufficient water storage is expected to exist within all the tree-available water-source pools (that is, soil zone, unsaturated zone, and saturated or groundwater zone) for tree uptake and growth, leading to a significant increase in the width of annual growth rings in the tree (shown with hypothetical tree-ring of circular shape here). B and d show conditions of drought-induced water stress (DIWS) and tunneling-induced water stress (TIWS), respectively. C and e show the recovery conditions of DIWS and TIWS during or after a long wet period, respectively. Both DIWS (b) and TIWS (d) have similar effects on the width of annual growth rings in the tree (causing a significant narrowing in the tree-ring width; shown with hypothetical tree-ring of elongated oval shape here). However, the intensity and duration of water stress induced by them are not the same on the whole hydrological system. Therefore, they may have varying adverse effects on tree growth dynamics and function under changing climate conditions. As shown in panel b, drought may significantly reduce water storage in tree-available water-source pools, but gradually (and over a long period compared to tunneling). Thus, the shallower and deeper water-source pools are exposed to higher and lower vulnerability, respectively. For example, during a period of drought, as shown in panel b, the intensity of the effects of DIWS on the soil zone is far more substantial and more widespread than on the groundwater zone. Consequently, due to approaching the moisture level of the soil zone to a threshold or wilting point, sufficient soil water storage may not be available for tree uptake and growth (Feldman et al., 2018; Gokdemir et al., 2019). As demonstrated in panel c, with the mediation of long-term favorable climatic (wet) conditions, DIWS may be fully recovered, leading to a complete recovery in the growth level of the tree (shown with hypothetical tree-ring of circular shape here). As indicated in panel d, tunneling can promptly and dramatically deplete all the shallow and deep water-source pools altogether at the very beginning of the excavation phase (Gokdemir et al., 2019; Liu et al., 2019). However, the deeper pools are exposed to higher vulnerability than the shallower ones (Liu et al., 2019; Lv et al., 2020). For example, during or shortly after an event of tunneling, as shown in panel d, the intensity of the effects of TIWS on the groundwater zone is far stronger and more widespread than on the soil zone, which will lead to a significant decrease in water uptake from the groundwater pool for tree use and growth because of poor water storage in this zone than the soil zone. As shown in panel e, with the mediation of long-term favorable climatic (wet) conditions, TIWS may be partially (but not completely) recovered, subsequently leading to an incomplete recovery in the growth level of the tree (shown with hypothetical tree-ring of rounded oval shape here).

evidence of ecohydrological (negative) effects associated with TIGD and the TIGD-linked water losses of other forest trees-available water sources. Our findings indicate that forest stands living in any landscape, particularly in the karst landscapes (known as delicate landscapes), can be highly vulnerable to tunneling-induced water stress. The magnitude of vulnerability to such water stress may be far more severe than drought-induced water stress. It brings about the growth dynamics of forest trees gradually weakening over time, which will likely never be fully restored even under the best (long-term infrequent) wet circumstances. Based on our findings, it is highly recommended that in future investigations, researchers should explore the ecohydrological effects associated with tunneling-induced water losses across tunnel-affected forest ecosystems, primarily over long-term intervals. To achieve this goal, the annual growth rings of the tree stands are the most powerful and cost-effective tool to be applied. The findings of this study can serve as a preliminary guide for forest and groundwater conservation and management at the regional, national, and global scales. Researchers can rely on them for future investigations to address and quantify individual (from a short-term perspective) and aggregated (from a long-term perspective) ecohydrological effects resulting from (climate-mediated) anthropogenic interventions such as tunneling within the stand and landscape scales of each similar (tunnel-affected) forest ecosystem around the world.

## Declaration of competing interest

The authors declare that they have no known competing financial interests or personal relationships that could have appeared to influence the work reported in this paper.

## Acknowledgements

This research was supported by the National Key Research and Developmental Program of China (2016YFC0502306), the Open Project Program of Chongqing Key Laboratory of Karst Environment (Cqk202003), and the Chongqing Municipal Science and Technology Commission Fellowship

Fund (CSTC2019yszx-jcyjX0002, CSTC2020yszx-jcyjX0006). The data that support the findings of this study are available from the corresponding author upon reasonable request.

## CRediT authorship contribution statement

**Hamid M. Behzad:** Conceptualization, Visualization, Methodology, Data curation, Software, Formal analysis, Writing- Original draft preparation, Writing- Reviewing and Editing.

**Yongjun Jiang:** Supervision, Project administration, Funding acquisition, Conceptualization, Visualization, Methodology, Writing- Reviewing and Editing.

**Muhammad Arif:** Visualization, Methodology, Writing- Reviewing and Editing.

**Chao Wu, Qiufang He, Haijuan Zhao, Tongru Lv:** Resources, Sampling, Investigation.

## Appendix A. Supplementary data

Supplementary data to this article can be found online at https://doi.org/10.1016/j.scitotenv.2021.152375.

## References


Anderegg, W.R.L., Anderegg, L.D.L., 2012. Hydraulic and carbohydrate changes in experimental drought induced mortality of saplings in two conifer species. Tree Physiol. 33, 252–260.

Attanayake, P.M., Waterman, M.K., 2006. Identifying environmental impacts of underground construction. Hydrogeol. J. 14, 1160–1170.

Banzato, C., Civita, M.V., Fiorucci, A., Vigna, B., Papale, S., 2011. Hydrogeological prognosis with regard to realisation of the new Colle Di Tenda road tunnel. Am. J. Environ. Sci. 7, 1–14.

Barbeta, A., Mejía-Chang, M., Ogaya, R., Voltas, J., Dawson, T.E., Peñuelas, J., 2015. The combined effects of a long-term experimental drought and an extreme drought on the use of plant-water sources in a mediterranean forest. Glob. Chang. Biol. 21, 1213–1225.

Barichivich, J., Peylin, P., Launois, T., Daux, V., Risi, C., Jeong, J., Luyssaert, S., 2021. A triple tree-ring constraint for tree growth and physiology in a global land surface model. Biogeosciences 18, 3781–3803.

Berdanier, A.B., Clark, J.S., 2018. Tree water balance drives temperate forest responses to drought. Ecology 99, 506–2514.

Bigler, C., Veblen, T.T., 2009. Increased early growth rates decrease longevities of conifers in subalpine forests. Oikos 118, 1130–1138.

Biondi, F., Strachan, S., 2012. Dendrohydrology in 2050: challenges and opportunities. In: Grayman, W.M., Loucks, D.P., Saito, L. (Eds.), Toward a Sustainable Water Future: Visions for 2050. American Society of Civil Engineers, pp. 355–362.

Biondi, F., Waikul, K., 2004. DENDROCLIM2002: a C++ program for statistical calibration of climate signals in tree-ring chronologies. Comput. Geosci. 30, 303–311.

Bogino, S.M., Jobbágy, E.G., 2011. Climate and groundwater effects on the establishment, growth and death of Prosopis caldenia trees in the Pampas (Argentina). For. Ecol. Manag. 262, 1766–1774.

Bonacci, O., Pipan, T., Culver, D.C.A., 2009. Framework for karst ecohydrology. Environ. Geol. 56, 891–900.

Bowman, D., Brienen, R., Gloor, E., Phillips, O.L., Prior, L.D., 2013. Detecting trends in tree growth: not so simple. Trends Plant Sci. 18, 11-17.

Bradley, K.L., Pregitzer, K.S., 2007. Ecosystem assembly and terrestrial carbon balance under elevated $CO_2$. Trends Ecol. Evol. 22, 538–547.

Breitenmoser, P., Brönnimann, S., Frank, D., 2014. Forward modelling of tree-ring width and comparison with a global network of tree-ring chronologies. Clim. Past 10, 437–449.

Briffa, K.R., Jones, P.D., Schweingruber, F.H., Karlen, W., Shiyatov, S.G., 1996. Tree-ring variables as proxy-climate indicators: problems with low-frequency signals. In: Jones, P.D., Bradley, R.S., Jouzel, J. (Eds.), Climate Variations and Forcings Mechanisms of the Last 2000 Years. Springer, Berlin, pp. 9–41.

Butscher, C., Huggenberger, P., Zechner, E., 2011. Impact of tunneling on regional groundwater flow and implications for swelling of clay-sulfate rocks. Eng. Geol. 117, 198–206.

Cao, M., Wu, C., Liu, J., Jiang, Y., 2020. Increasing leaf $\delta^{13}C$ values of woody plants in response to water stress induced by tunnel excavation in a karst trough valley: implication for improving water-use efficiency. J. Hydrol. 586, 124895.

Casagrande, G., Cucchi, F., Zini, L., 2005. Hazard connected to railway tunnel construction in karstic area: applied geomorphological and hydrogeological surveys. Nat. Hazards Earth Syst. Sci. 5, 243–250.

Celico, P., Fabbrocino, S., Petitta, M., Tallini, M., 2005. Hydrogeological impact of the Gran Sasso motor-way tunnels (Central Italy). Giornale di Geologia Applicata 1, 157–165.

Cesano, D., Olofsson, B., Bagtzoglou, A.C., 2000. Parameters regulating groundwater inflows into hard rock tunnels – a statistical study of the Bolmen tunnel in southern Sweden. Tunn. Undergr. Space Technol. 15, 153–165.

Chae, G.T., Yun, S.T., Choi, B.Y., Yu, S.Y., Jo, H.Y., Mayer, B., Kim, Y.J., Lee, J.Y., 2008. Hydrochemistry of urban groundwater, Seoul, Korea: the impact of subway tunnels on groundwater quality. J. Contam. Hydrol. 101, 42–52.

Chen, K.L., Wu, H.N., Cheng, W.C., Zhang, Z., Chen, J., 2017. Geological characteristics of strata in Chongqing, China, and mitigation of the environmental impacts of tunneling-induced geo-hazards. Environ. Earth Sci. 76, 1–16.

Chiu, Y.C., Chia, Y., 2012. The impact of groundwater discharge to the Hsueh-Shan tunnel on the water resources in Northern Taiwan. Hydrogeol. J. 20, 1599–1611.

Cook, E.R., 1985. A Time Series Analysis Approach to Tree-ring Standardization.. PhD DissertationThe University of Arizona, Tucson.

Cook, E.R., Briffa, K.R., 1990. A comparison of some tree-ring standardization methods. In: Cook, E.R., Kairiukstis, L.A. (Eds.), Methods of Dendrochronology: Applications in the Environmental Sciences. Kluwer Academic Publishers, Dordrecht, pp. 153–162.

Cook, E.R., Briffa, K.R., Meko, D.M., Graybill, D.A., Funkhouser, G., 1995. The 'segment length curse' in long tree-ring chronology development for paleoclimatic studies. Holocene 5, 229–237.

Creutzfeldt, B., Heinrich, I., Merz, B., 2015. Total water storage dynamics derived from tree-ring records and terrestrial gravity observations. J. Hydrol. 529, 640–649.

Dogan, S., Berktay, A., Singh, V.P., 2012. Comparison of multi-monthly rainfall-based drought severity indices, with application to semi-arid Konya closed basin, Turkey. J. Hydrol. 470–471, 255–268.

Duchesne, L., Ouimet, R., Morneau, C., 2003. Assessment of sugar maple health based on basal area growth pattern. Can. J. For. Res. 33, 2074–2080.

Edvardsson, J., Hansson, A., 2015. Multiannual hydrological responses in Scots pine radial growth within raised bogs in southern Sweden. Silva Fenn 49, 1–14.

Ehleringer, J.R., Dawson, T.E., 1992. Water uptake by plants: perspectives from stable isotope composition. Plant Cell Environ. 15, 1073–1082.

Estrada-Medina, H., Graham, R.C., Allen, M.F., Jimenez-Osornio, J.J., Robles-Casolco, S., 2013. The importance of limestone bedrock and dissolution karst features on tree root distribution in northern Yucatan, Mexico. Plant Soil 362, 37–50.

Fan, Y., Miguez-Macho, G., Jobbágy, E.G., Jackson, R.B., Otero-Casal, C., 2017. Hydrologic regulation of plant rooting depth. Proc. Natl. Acad. Sci. U. S. A. 114, 10572–10577.

Fekedulegn, D., Hicks, R.R., Colbert, J.J., 2003. Influence of topographic aspect, precipitation and drought on radial growth of four major tree species in an Appalachian watershed. For. Ecol. Manag. 177, 409–425.

Feldman, A.F., Gianotti, D.J.S., Konings, A.G., McColl, K.A., Akbar, R., Salvucci, G.D., Entekhabi, D., 2018. Moisture pulse-reserve in the soil-plant continuum observed across biomes. Nat Plants 4, 1026–1033.

Ferguson, G., George, S.S., 2003. Historical and estimated groundwater levels near Winnipeg, Canada, and their sensitivity to climate variability. J. Am. Water Resour. Assoc. 39, 1249–1259.

Fkiri, S., Guibal, F., Fady, B., Khorchani, A.E., Khaldi, A., Khouja, M.L., Nasr, Z., 2018. Tree-rings to climate relationships in nineteen provenances of four black pines sub-species (Pinus nigra Arn.) growing in a common garden from Northwest Tunisia. Dendrochronologia 50, 44–51.

Ford, D.C., Williams, P.W., 2007. Karst Hydrogeology and Geomorphology. Wiley, Chichester.

Fritts, H.C., 1976. Tree Rings and Climate. Academic Press, London.

Gao, S., Liu, R., Zhou, T., Fang, W., Yi, C., Lu, R., Zhao, X., Luo, H., 2018. Dynamic responses of tree-ring growth to multiple dimensions of drought. Glob. Chang. Biol. 24, 5380–5390.

Gokdemir, C., Rubin, Y., Li, X., Li, Y., Xu, H., 2019. Vulnerability analysis method of vegetation due to groundwater table drawdown induced by tunnel drainage. Adv. Water Resour. 133, 103406.

Grace, J., Berninger, F., Nagy, L., 2002. Impacts of climate change on the tree line. Ann. Bot. 90, 537–544.

Grissino-Mayer, H.D., 2001. Evaluating crossdating accuracy: a manual and tutorial for the computer program COFECHA. Tree-Ring Res 57, 205–221.

Hann, D.W., Larsen, D.R., 1991. Diameter growth equations for fourteen tree species in southwest Orego. Research Bulletin 69. University, Oregon State.

Helama, S., Lindholm, M., Timonen, M., Eronen, M., 2004. Detection of climate signal in dendrochronological data analysis: a comparison of tree-ring standardization methods. Theor. Appl. Climatol. 79, 239–254.

Holmes, R.L., 2001. Dendrochronology program library. Available from the Laboratory of Tree Ring Research. University of Arizona, Tucson, AR, USA . https://www.ltrr.arizona.edu/software.html.

Jump, A.S., Hunt, J., Peñuelas, J., 2006. Rapid climate change-related growth decline at the southern range edge of Fagus sylvatica. Glob. Chang. Biol. 12, 2163–2174.

Kolymbas, D., Wagner, P., 2007. Groundwater ingress to tunnels: the exact analytical solution. Tunn. Undergr. Space Technol. 22, 23–27.

Kukarskih, V.V., Devi, N.M., Surkov, A.Y., Bubnov, M.O., Gorlanova, L.A., Ekba, Y.A., Hantemirov, R.M., 2020. Climatic responses of Pinus brutia along the Black Sea coast of Crimea and the Caucasus. Dendrochronologia 64, 125763.

LeBlanc, D.C., Nicholas, N.S., Zedaker, S.M., 1992. Prevalence of individual-tree growth decline in red spruce populations of the southern Appalachian mountains. Can. J. For. Res. 22, 905–914.

Lebourgeois, F., Breda, N., Ulrich, E., Granier, A., 2005. Climate-tree growth relationships of European beech (Fagus sylvatica L.) in the French Permanent Plot Network (RENECOFOR). Trees 19, 385–401.

Lei, S., Bian, Z., Daniels, J.L., He, X., 2010. Spatio-temporal variation of vegetation in an arid and vulnerable coal mining region. Int. J. Min. Sci. Technol. 20, 485–490.

Levesque, M., Saurer, M., Siegwolf, R., Eilmann, B., Brang, P., Bugmann, H., Rigling, A., 2013. Drought response of five conifer species under contrasting water availability suggests high vulnerability of Norway spruce and European larch. Glob. Chang. Biol. 19, 3184–3199.

Li, H., Kagami, H., 1997. Groundwater level and chemistry changes resulting from tunnel construction near Matsumoto City. Environ. Geol. 31, 76–84.

Li, L., Tu, W., Shi, S., Chen, J., Zhang, Y., 2016. Mechanism of water inrush in tunnel construction in Karst area. Geomat. Nat. Haz. Risk 7, 35–46.

Li, X., Li, Y., Chang, C.F., Benjamin, T., Ziyang, C., Jon, S., Changhong, W., Rubin, Y., 2018. Stochastic, goaloriented rapid impact modeling of uncertainty and environmental impacts in poorly sampled sites using ex-situ priors. Adv. Water Resour. 111, 174–191.

Li, J., Hong, A., Yuan, D., Jiang, Y., Deng, S., Cao, C., Liu, J., 2020. A new distributed karst-tunnel hydrological model and tunnel hydrological effect simulations. J. Hydrol. 593, 125639.

Lima, R.P.C., Silva, D.D.D., Moreira, M.C., Passos, J.B.M.C., Coelho, C.D., Elesbon, A.A.A., 2019. Development of an annual drought classification system based on drought severity indexes. An. Acad. Bras. Cienc. 91, 1–11.

Lin, Y.S., Medlyn, B.E., Duursma, R.A., Prentice, I.C., Wang, H., Baig, S., Eamus, D., Dios, V.R.D., 2015. Optimal stomatal behaviour around the world. Nat. Clim. Chang. 5, 459–464.

Liu, J., Shen, L., Wang, Z., Duan, S., Wu, W., Peng, X., Wu, C., Jiang, Y., 2019. Response of plants water uptake patterns to tunnels excavation based on stable isotopes in a karst trough valley. J. Hydrol. 571, 485–493.

Lloyd, A.H., 1997. Response of tree-line populations of foxtail pine (Pinus balfouriana) to climate variation over the last 1000 years. Can. J. For. Res. 27, 936–942.

Loaiciga, H.A., Haston, L., Michaelsen, J., 1993. Dendrohydrology and long-term hydrologic phenomena. Rev. Geophys. 31, 151–171.

Lv, Y., Jiang, Y., He, W., Cao, M., Mao, Y., 2020. A review of the effects of tunnel excavation on the hydrology, ecology, and environment in karst areas: current status, challenges, and perspectives. J. Hydrol. 586, 124891.

Millar, C.I., Westfall, R.D., Delany, D.L., Bokach, M.J., Flint, A.L., Flint, L.E., 2012. Forest mortality in high-elevation whitebark pine (Pinus albicaulis) forests of eastern California, USA; influence of environmental context, bark beetles, climatic water deficit, and warming. Can. J. For. Res. 765, 749–765.

Mohan, J.E., Clark, J.S., Schlesinger, W.H., 2004. Genetic variation in germination, growth, and survivorship of red maple in response to subambient through elevated atmospheric $CO_2$. Glob. Chang. Biol. 10, 233–247.

Mossmark, F., Ericsson, L.O., Norin, M., Dahlström, L.O., 2015. Hydrochemical changes caused by underground constructions-a case study of the Kattleberg rail tunnel. Eng. Geol. 191, 86–98.

Muzika, R.M., Guyette, R.P., Zielonka, T., Liebhold, A.M., 2004. The influence of $O_3$, $NO_2$ and $SO_2$ on growth of Picea abies and Fagus sylvatica in the Carpathian mountains. Environ. Pollut. 130, 65–71.

Obojes, N., Meurer, A., Newesely, C., Tasser, E., Oberhuber, W., Mayr, S., Tappeiner, U., 2018. Water stress limits transpiration and growth of European larch up to the lower subalpine belt in an inner-alpine dry valley. New Phytol. 220, 460–475.

Pedersen, B.S., 1998. The role of stress in the mortality of Midwestern oaks as indicated by growth prior to death. Ecology 79, 79–93.

Peñuelas, J., Hunt, J.M., Ogaya, R., Jump, A.S., 2008. Twentieth century changes of tree-ring $\delta^{13}C$ at the southern range-edge of Fagus sylvatica: increasing water-use efficiency does not avoid the growth decline induced by warming at low altitudes. Glob. Chang. Biol. 14, 1076–1088.

Perez-Valdivia, C., Sauchyn, D., 2011. Tree-ring reconstruction of groundwater levels in Alberta, Canada: long term hydroclimatic variability. Dendrochronologia 29, 41–47.

Perrochet, P.A., 2005. Simple solution to tunnel or well discharge under constant drawdown. Hydrogeol. J. 13, 886–888.

Phillips, O.L., Heijden, G.V.D., Lewis, S.L., López-González, G., Aragão, L.E.O.C., Lloyd, J., Malhi, Y., Monteagudo, A., 2010. Drought-mortality relationships for tropical forests. New Phytol. 187, 631–646.

Phipps, R.L., Whiton, J.C., 1988. Decline in long-term growth trends of white oak. Can. J. For. Res. 18, 24–32.

Pujades, E., Vazquez-Sune, E., Culi, L., Carrera, J., Ledesma, A., Jurado, A., 2015. Hydrogeological impact assessment by tunnelling at sites of high sensitivity. Eng. Geol. 193, 421–434.

Rodríguez-Catón, M., Villalba, R., Srur, A.M., Luckman, B., 2015. Long-term trends in radial growth associated with Nothofagus pumilio forest decline in Patagonia: integrating local- into regional-scale patterns. For. Ecol. Manag. 339, 44–56.

Rong, L., Chen, X., Chen, X.H., Wang, S.J., Du, X.L., 2011. Isotopic analysis of water sources of mountainous plant uptake in a karst plateau of southwest China. Hydrol. Process. 25, 3666–3675.

Rozendaal, D.M.A., Brienen, R.J.W., Soliz-Gamboa, C.C., Zuidema, P.A., 2010. Tropical tree rings reveal preferential survival of fast-growing juveniles and increased juvenile growth rates over time. New Phytol. 185, 759–769.

Schuster, R., Oberhuber, W., 2013. Drought sensitivity of three co-occurring conifers within a dry inner Alpine environment. Trees 27, 61–69.

Stokes, M.A., Smiley, T.L., 1996. An Introduction to Tree-ring Dating. University of Arizona Press.

Tamkeviciute, M., Edvardsson, J., Pukiene, R., Taminskas, J., Stoffel, M., Corona, C., Kibirkštis, G., 2018. Scots pine (Pinus sylvestris L.) based reconstruction of 130 years of water table fluctuations in a peatland and its relevance for moisture variability assessments. J. Hydrol. 558, 509–519.

Vincenzi, V., Gargini, A., Goldscheider, N., 2009. Using tracer tests and hydrological observations to evaluate effects of tunnel drainage on groundwater and surface waters in the Northern Apennines (Italy). Hydrogeol. J. 17, 135–150.

Vincenzi, V., Gargini, A., Goldscheider, N., Piccinini, L., 2014. Differential hydrogeological effects of draining tunnels through the Northern Apennines, Italy. Rock Mech. Rock Eng. 47, 947–965.

Wang, X., Pederson, N., Chen, Z., Lawton, K., Zhu, C., Han, S., 2019. Recent rising temperatures drive younger and southern korean pine growth decline. Sci. Total Environ. 649, 1105–1116.

Wu, Z., Behzad, H.M., He, Q., Wu, C., Bai, Y., Jinag, Y., 2021. Seasonal transpiration dynamics of evergreen ligustrum lucidum linked with water source and water-use strategy in a limestone karst area, southwest China. J. Hydrol. 597, 126199.

Yang, J., Nie, Y.P., Chen, H.S., Wang, S., Wang, K.L., 2016. Hydraulic properties of karst fractures filled with soils and regolith materials: implication their ecohydrological functions. Geoderma 276, 93–101.

Yu, D., Liu, J., Benard, J.L., Zhou, L., Zhou, W., Fang, X., Wei, Y., Jiang, S., Dai, L., 2013. Spatial variation and temporal instability in the climate-growth relationship of Korean pine in the Changbai Mountain region of Northeast China. For. Ecol. Manag. 300, 96–105.

Zeng, C.F., Zheng, G., Zhou, X.F., Xue, X.L., Zhou, H.Z., 2019. Behaviours of wall and soil during pre-excavation dewatering under different foundation pit widths. Comput. Geotech. 115, 103169.

Zhao, Y., Li, P.F., Tian, S.M., 2013. Prevention and treatment technologies of railway tunnel water inrush and mud gushing in China. J. Rock Mech. Geotech. Eng. 5, 468–477.

Zheng, W., Wang, X., Tang, Y., Liu, H., Wang, M., Zhang, L., 2017. Use of tree rings as indicator for groundwater level drawdown caused by tunnel excavation in Zhongliang Mountains, Chongqing, Southwest China. Environ. Earth Sci. 76, 1–14.

Zweifel, R., Zimmermann, L., Zeugin, F., Newbery, D.M., 2006. Intra-annual radial growth and water relations of trees: implications towards a growth mechanism. J. Exp. Bot. 57, 1445–1459.